doi.org/10.36721/PJPS.2021.34.5.SUP.1837-1847.1

Biosynthesis of silver nanoparticles from *Mukia maderaspatana* (L) and their biological activities

Noreen Samad[1]*, Saba Farooq[1], Saima Khaliq[2], Saara Ahmed[3], Mehtab Alam[4], Sana Mustafa[5], Azizuddin[5], Uzma Raza[6] and Wajahat Nadeem[2]

[1]Department of Biochemistry, Bahauddin Zakariya University, Multan, Pakistan
[2]Department of Biochemistry, Federal Urdu University of Arts, Science and Technology, Karachi, Pakistan
[3]Department of Biological and Biomedical Sciences, The Aga Khan University, Karachi, Pakistan
[4]Department of Biochemistry, Azad Jammu Kashmir Medical College, Muzaffarabad, Azad Kashmir, Pakistan
[5]Department of Chemistry, Federal Urdu University of Arts, Science and Technology, Karachi, Pakistan
[6]Department of Biochemistry, Hamdard Medical College, Hamdard University, Karachi, Pakistan

Abstract: Nanotechnology is a field of science that consists of atoms, molecules and supramolecular molecules that create nanoparticles ranging in size from 1-100nm. Silver nanoparticles are widely used that are considered as effective antimicrobial agents. In this paper, the antioxidant activity of biosynthesized SNPs were analyzed by the DPPPH activity, hydrogen peroxide activity, hydroxyl RSA, TAC, TFC; their results confirmed that the phenolic compounds of this plant peels extracts enhanced the antioxidant and antiglycation activity with respect to silver nanoparticles. Biosynthesized nanoparticles of this plant extracts also showed strong zone of inhibition against the different Xanthomas, Pseudomonas and *E. coli*. This study concluded that biosynthesized nanoparticles of *Mukia maderaspatna* (M.M) plant peels extracts have the great biological activities i.e. antiglycation, antioxidant and antibacterial. More research is needed to know the exact dose rate and to compare the different dose combination of the plant with the strong antibiotic agents against these bacteria.

Keywords: Nanotechnology, *Mukia maderaspatna*, antioxidants, antigylcation, antibacterial.

INTRODUCTION

Nanotechnology is a field of science that consist of atoms, molecules and supramolecular molecules that create nanoparticles ranging in size from 1-100nm (Shah *et al*., 2015). Nanoparticles (NPs) are considered as basic unit of nanotechnology (Dadfar *et al.,* 2019). They have wide range of physical and chemical functions due to their large surface area to volume ratio that are useful for antimicrobial and antioxidant activity (Moodley *et al*., 2018). Nanotechnology is an innovative skill for the synthesis of NPs having unique structural, biological and optical properties (Sabourian *et al*., 2020) that have the main role in health and medical applications i.e. drug delivery, biosensors (Zhang 2020), control the cell proliferation rate (Arsenopoulou *et al*., 2018), inhibit infection growth and regulate the body's abnormal molecular mechanism (Sarkar *et al*., 2018).

Nanoparticles, i.e. natural and engineered NPs, are of two forms depending on their Synthesis and Origin. Engineered nanoparticles are divided into two classes, called (1) organic NPs, (2) inorganic and metal inorganic NPs (Liu, 2006). Metallic nanoparticles have the diverse physiochemical properties as these have numerous applications i.e. health care, synthetic biology and cellular transportation (Shaik *et al*., 2018). Gold, silver and platinum are the main derivative of metallic NPs that have pharmaceutical applications. These metallic particles' properties depend on their size, their morphology and their surface load using advanced microscoping techniques such as microscopy of the atomic strength (AFM), microscopic electron scanning (SEM) and electron transmission microscopy (EMT) (Bhatia, 2016). However, the use of silver is known to be an important antimicrobial agent with low human toxicity (Perugu *et al*., 2016). Tumors or rheumatoid arthritis can be treated with silver NPs (SNPs) that can be used as carriers for the transmission of drugs and genes (Lin *et al*., 2015). SNPs have significant antimicrobial activity, as used for medical devices and optical device, biotechnological electronics and catalytic science, due to their small scale, spherical form and high surface-to-volume ratios. (Qidwai *et al*., 2018). The silver is a soft, white and shiny metal that has high thermal and electrical conductivity that is used against infectious diseases and surgical diseases (Firdhouse *et al*., 2015).

Green chemistry has a main role for the synthesis of nanomaterials using plant extracts that are non-toxic, safe and environment friendly as they contain natural coating against the pathogens (Khan *et al*., 2018). Plants crude extracts i.e. seeds, leaves and flowers contain metabolites such as phenolic acid, flavonoids, alkaloids and terpenoids (Kuppusamy *et al*., 2016). Those extracts have reducing property as to reduce ions into bulk metallic eco-friendly NPs formation (Shaik *et al*., 2018). These are the

**Corresponding author:* e-mail: noreen.samad@bzu.edu.pk

main constituents to act as reducing or antioxidant activity, antimicrobial and antiglycation activity of medicinal plants, fruits or vegetables (Ahmed *et al*., 2016). Metal NPs of plants extracts are cost effective so these are economically valuable alternative for the production of NPs at large scale (Soares *et al*., 2018).

Mukia maderaspatana (M.M) (L.) plant belongs to family Cucurbitaceae is a leafy vegetable, an annual monoecious tender climber. It is found in the south Indian and Pakistani region and the tropics and sub tropics of the old world (Chitra *et al*. 2015). Several plant based biosynthesized SNPs are reported early. But the M.M. plant based SNPs are also reported too as it has high contents of phenolic compounds that have medicinal properties i.e. antibacterial, analgesic, stimulant and anti-inflammatory (Srilatha *et al*., 2014). M.M. is anticancer, anti-inflammatory, and anti-diabetes methane extract from the entire plant and the ethanol and aqueous extracts are antihyperglycemia. However, an antiulcer is aqueous extract of the leaves (Petrus, 2013). Devi *et al*., (2016) have claimed that the vast number of metabolites which play a major function in the reduction of gold and silver ions in each section of the plant reduces bronchitis, fiver and stomach issues. In the same way (Chitra *et al*., 2015) SNPs were produced from aqueous extract from M.M. They showed a dominant power over malary vectors.

No research study has been done to identify the antioxidant, antiglycation and antimicrobial activity of peels extracts of M.M. So our aim of study was to prepare the nanoparticles of peels extracts through silver NPs and to identify the antimicrobial activity and antiglycation activity of M.M. (L.) Pure peels extracts with respect to silver nano particles and to compare their activities with respect to SNPs. The biosynthesized SNPs were systematically characterized by UV-visible spectroscopy, Scanning electron microscope, Fourier transform Infrared Spectroscopy (FTIR) and Electron Diffraction X-RAY.

MATERIALS AND METHODS

Collection and identification of plant

The fruit of M.M. was gathered in the Lodhran district, Pakistan. The voucher number for the identification for the plant was listed as R.R. Stewart F.W.Pak 706 and issued by Dr Zafar-ul-Zafar, Institute of Pure and Applied Biology Department, Bahauddin Zakariya University of Multan, Pakistan.

Washing, grinding and preparation of peels extracts

To remove any contamination, the fruits were washed with water, peeled, and dried. Following that grinded by electrical grinding machine to get fine powder. Four types of extracts methanol (Balouiri *et al*., 2016), ethanol (Chang *et al*., 2001), acetone (Gurunathan *et al*., 2013) were made using the maceration method, while the water extract was made using the decoction method (Logeswari *et al*., 2015).

Biosynthesis of SNPs

In four beakers, 10 ml of each extract was taken. In each beaker, 50 ml of 1 mMAgNO3 solution were added, coated with aluminum foils and held at normal temperature 24 hours in the dark. The colour of the solutions turned from yellow to dark brown following the bio-reduction process that revealed the SNP synthesis. The SNPs were centrifuged at 6000 RPM, and the silver nanoparticles were filtered for 20 minutes. They were then washed with purified water to dissolve infinite spores. The colloidal washing fluid was used for the characterization and other biological behavior (McPherson *et al*., 1988).

Characterization of biosynthesized SNPs

a. UV Spectrophotometry

Aliquot of 100 µl of samples in the UV cell for testing absorption was expected to possess organically reduced (water and alcoholic *Mukia Maderaspatana* extracts containing SNPs). The UV Perkin-Elmer Lambda spectrophotometer with a wavelength of 400 nm to 450 nm showed maximum emission.

b. Scanning Electron Microscope (SEM)

On the slide surface, filled with a platinum sheet, some drops of the sample were added as platinum works as a conductor. And the slide was dried in the air. The sample was then analyzed by SEM. The result of this study was a high-resolution photograph. The sample was crossed by a beam of electrons. Magnetic lenses based on the electron beam are used. The interaction between electrons and the sample surface gives the picture of NPs.

c. Fourier Transform Infrared Spectroscopy (FTIR) analysis,

At 700C, the samples were kept. The dried samples have then been added to the KBr matrix. The samples were passed via IRR. Any of these radiations is absorbed by samples. The other was distributed. In this procedure, KBr function as control. The group analysis was performed approximately 4000–600 cm−1. Elemental M.M plant analysis was carried out using FT-IR. The chemical bonding in the sample shows strained or bent as the infra-red rays came into the sample.

d. Electron Diffraction X-RAY (EDX)

EDX was used to evaluate various sample components. The procedure took place at 20 KeV. The sample percentage of Ag was obtained by EDX. The sample was made on a foil of aluminum. On the foil, supernatant was dropped. The foil was then dried. Aluminum foil stops the light sample. The sample obtained a different proportion of different elements.

Antioxidant Analysis

a. (DPPH (Radical Scavenging Activity),

One ml of each extract was mixed in 2 mL of DPPH solution and their corresponding NPs. The tubes have been sealed by aluminum foil. The mixture was kept in the dark for 30 minutes. A.A acts as a reference substance. At 517nm, each extract and its respective NPs were absorbed. The percentage age of inhibition was estimated using the following equation.

*%age inhibition = [ABo – AB1 / ABo] * 100 ... (1)*

Where ABo displayed power absorption. AB1 was sample absorption coefficient. Each extract's DPPH activity was seen in percentage (Mehta *et al*., 2017).

b. Hydroxyl Radical Scavenging Activity

One ml of each extract was combined with 1 ml of ferrous sulphate and 1 ml of sodium salicylate, respectively NP. The process began by adding 1ml of hydrogen peroxide. The mixture was preserved in darkness for 30 minutes at 370C. Control was increased by placing the same amount of ferrous sulphate and sodium salicylate. Each sample was absorbed at 510nm against blank. The behavior of hydroxyl was calculated by formula indicated in equation (1)

c. TAC by Phosphomolybdenum assay

Sulpuric acid, ammonium moly date and phosphate buffer of equivalent volume is combined with the preparation of a reaction mix. In the test tubes, inject 1 ml of each extract and each of its NPs and 3 ml of the response mixture. The aluminum foil was used for test pipes. These test tubes) had 90) minutes of incubation at 950C. At room temperature, every test solution was cooled down. (Each solution's concentration at 695 nm with blank was measured. As regulation, G.A. was taken. The phosphomolybdenum test has been computed using the equation formula (1)

d. Hydrogen peroxide Radical Scavenging Activity

In each tube of the test, 40 mm solution of H2O2 has been formulated (phosphate buffer with 7,4 pH. 8 tubes have been taken. 3,4 ml respective of each extract and nanoparticle colloidal fluid have been added, while 0,6 ml of H2O2 solution has been added to every tube of the test. 10 minutes of tubing is held. Adding ascorbic acid solution (3.4 ml and H2O2 0.6 ml) was prepared by Norm. Spectrophotometrically, the solution was read at 230 nm by a white solution. (The inhibition percentage for each sample was calculated in an equation form (1)

Total Flavonoid Contents

In aluminum trichloride tubes add 2mL of each leaf extracts and the NPs and 2ml methanol in the test tubes. Both tubes were held for 10 minutes in the incubator. The concentration of all samples was eventually determined by norm at 430 nm with blank Quercetin. In comparison with normal, the absorption of each sample was assessed.

Antimicrobial Activity

The paper disk diffusion method has investigated the antimicrobial activity. In distilled water in conical flask, 2 grams of Yeast extract, 4 grams of NaCl, Tryptone and 8 Grams of Agar were added and agitated to obtain homogeneous blend. Discs were prepared from Whatman filters no. 1 by pinnacle and wrapped in a 3-hour aluminum foil (Ruch *et al*., 1989). These Bacterial stains *E. coli,* pseudomonas syringae and Xanthomonas were examined for antimicrobial activity. They have been collected from the pure and applied biology microbiology laboratory. The Petri plate was autoclaved. Every Petri plate has been added to the prepared media and can stand till the frost. The test with the help of an inoculation loop was distributed across the media. Afterwards the discs in each test tube were placed on the media. The disk with micro pipette held 40 micro liters of extract and their respective nanoparticles. The plates had been set at room temperature in the incubator for 24 hours. The zones were established after incubations. These areas have been measured in mm.

Antiglycation assays

The same amount of sodium azide and fructose in the phosphate buffer were induced into 4ml bovine serum albumin. Then in 8 measuring tubes add 3 ml of any sample and reaction mix. These test tubes were closely sealed and held at 370C in the incubator. The samples were processed for seven days in the incubator. To prepare the reaction combination Bovine serum albumin was combined with the fructose solution. In similar conditions, positive was preserved (Zargar *et al*., 2011). These incubated materials have been used by calculation of 2 factors for antiglycation estimation. A) Fructosamine estimate (b) Estimate of the Carbonyl Group.

Estimation of fructosamine

In the pH sodium carbonate buffer 10.35 prepare a Nitroblue tetrazolium (NBT) solution. Eight tubes with crude extracts and nanoparticles have been taken and labelled. In the marked test tube, apply 40 micro liters of the glycated sample and the above formulated NBT pH 10.35 positivity control solution. For 30 minutes, these samples were incubated at 370C. Following the incubation, each sample absorbed the blank solution at 530 nm. A positive regulation is albumin and the fructose solution. Crude extract and its respective NPs were calculated by formula in the equation (1)

Carbonyl group estimation

A beaker was filled with the same volume of Dinitrophenyl hydrazine and HCL. These are tagged eight test tubes. Add 0.5 ml of glyced albumin in each test tube with the same amount of positive control and the solution of dinitrophenyle hydrazine. The test tubing was held at 37^{o}C for 60 minutes in the incubator. 2 mL of Tricholoroacetic acid were added to every test tube after

60minutes of incubation. Protein accumulation was caused by tricholoroacetic acid. Ethanol washed off the precipitates. 1mL urea has been applied to each test tube after washing. The spectrophotometer was then taken into absorption of each sample. The glycemic compound inhibition percentage was determined by the following formula.

*%age inhibition = [ABo – AB1 / ABo] * 100*

Where ABo displays the positive control absorption value. AB1 is glycated albumin absorption samples.

STATISTICAL ANALYSIS

Data on antioxidant assays analyzed by paired sample T-test, while antimicrobial, carbonyl group and fructosamine assays analyzed by Two-way anova followed by Tukey's test. SPSS version 19.00 was used for all data. $p < 0.05$ considered as significant.

RESULTS

Usage of extracts for the formation of biosynthesized SNPs

M.M. plant was used for the biosynthesis of SNPs in various extracts (methanol, ethanol, acetone and water). The results showed that extracts had a yellowish green color before adding silver nitrate solution, after the addition of silver nitrate the color of solution was turned brown. It indicates the syntheses of SNPs. SNPs were verified by UV Vis spectroscopy, SEM, EDX, and FTIR.

UV-vis Spectrophotometryanalysis

The spectrum of biosynthesized SNPs from acetone, methanol, ethanol and water extracts of M.M. peels respectively were represented by figs. 1a-1d that showed the maximum absorbance at 430 nm, 440nm, 435nm and 420 nm respectively. These figs. showed absorbance at different wavelengths with respect to the material and its respective nanoparticle.

Scanning electron microscope (SEM) analysis

To evaluate the (morphology and size of biosynthesized SNPs, scanning electron microscope was used. Figs. 2a-2d demonstrates the spherical shape of biosynthesized SNPs and the nanoparticles that gave the desired size of SNPs were bounds with the surface protein.

(Fourier Transform Infrared Spectroscopy (FTIR) analysis

Figs. 3a-3d showed the spectrums of biosynthesized SNPs respectively from methanol, ethanol, acetone and water extracts of M.M. peel. The peaks at the different numbers were seen in these spectrums. These peaks showed that various functional groups were extended. Due to the vibrations of amine groups, the functional group has been extended.

Figs. 4a-4d illustrated the spectrum from EDX study of biosynthesized SNPs from ethanol, water, methanol and acetone extracts respectively. The percentage of elements in this spectrum was different. The percentage of silver, alumina, carbon and chlorine was identified. The presence of silver in the sample has been verified.

Antioxidant activity

Extracts of fig. 5a showed large DPPH free radicals scavenging percentages. DPPH free radical (crude extracts and their respective nPs) inhibitions percentages have been tested by a T-test (df=1,4). The data showed the significant difference of methanol and its respective nanoparticle ($t=-5.184$, $P<0.05$), acetone and its respective nanoparticle ($t=-14.33$, $P<0.05$), ethanol and its respective nanoparticle ($t=-14.252$, $P<0.05$) and water and its respective nanoparticle ($t=-5.363$, $P<0.05$). Nanoparticles of M.M. methanol extract have demonstrated significantly greater capacity for DPPH scraping among all the samples. There was a higher activity in the nanoparticles of all extracts than in crude.

Fig. 5b excerpts have shown a prominent percentage of free radicals of hydrogen peroxide. A pairing T test (df=1,4) assessed the percentage inhibition of the hydrogen peroxide free radical of radical extracts and their corresponding NPs. The data showed the significant difference of methanol and its respective nanoparticle ($t=-9.443$, $P<0.05$), acetone and its respective nanoparticle ($t=-24.087$, $P<0.05$), ethanol and its respective nanoparticle ($t=-8.072$, $P<0.05$) and water and its respective nanoparticle ($t=-7.414$, $P<0.05$). Of all the samples, M.M. nanoparticles of methanol extract have been significantly more likely than other to scavenge hydrogen peroxide. There has been a greater scavenging occurrence than crude oil extracts in nanoparticles of the extracts.

Fig. 5c extracts showed prominent scavenging percentage of hydroxyl free radicals. The paired T test (df=1,4) was used to determine the percentage inhibition of the hydroxyl radical of (crude extracts and their respective NPs. The data showed the significant difference of methanol and its respective nanoparticle ($t=-25.261$, $P<0.05$), acetone and its respective nanoparticle ($t=-6.976$, $P<0.05$), ethanol and its respective nanoparticle ($t=-5.674$, $P<0.05$) and water and its respective nanoparticle ($t=-11.529$, $P<0.05$). Nanoparticles of M.M. methanol extract showed significantly greater capability than other samples. The extract nanoparticles had higher scavenging activity than the crude extracts.

Fig. 5d extracts of the phosphomolybdate free radicals showed prominent scavenging percentage. A paired sample T test was used to determine the percentage inhibitions of phosphomolybdates free from radical crud extracts and their respective NPs (df=1,4). The data showed the significant difference of methanol and its respective nanoparticle ($t=-5.719$, $P<0.05$).

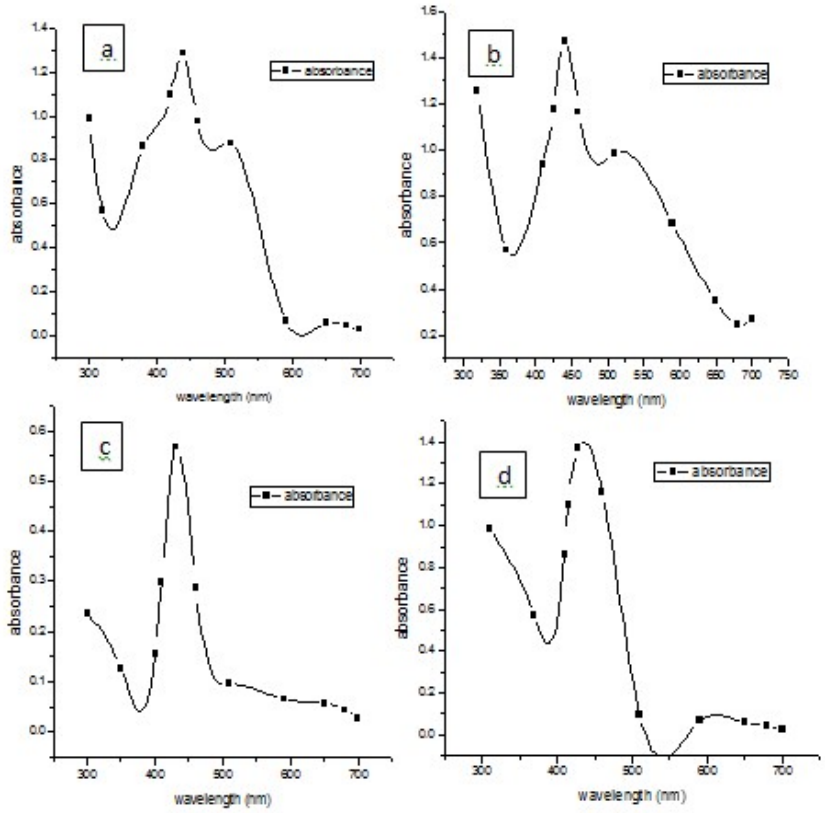

Fig. 1: UV vis absorption peak of biosynthesized SNPs (a) acetone extract, (b) methanol extract, (c) ethanol extract (d) water extract

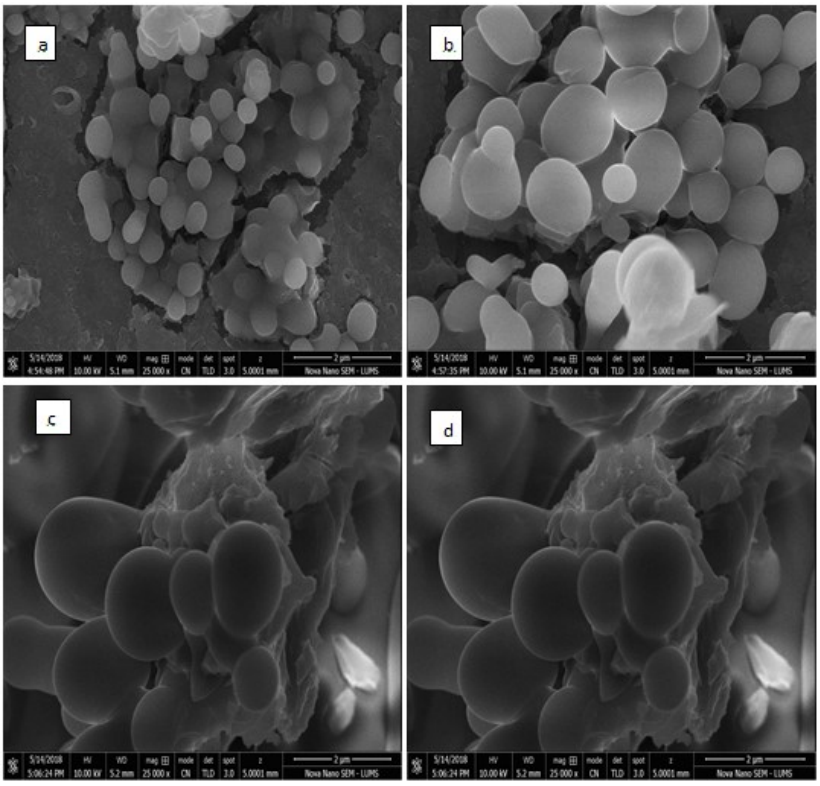

Fig. 2: Showed SEM image of biosynthesized SNPs (a) methanol extract,(b) ethanol extract, (c) acetone extract (d) water extract

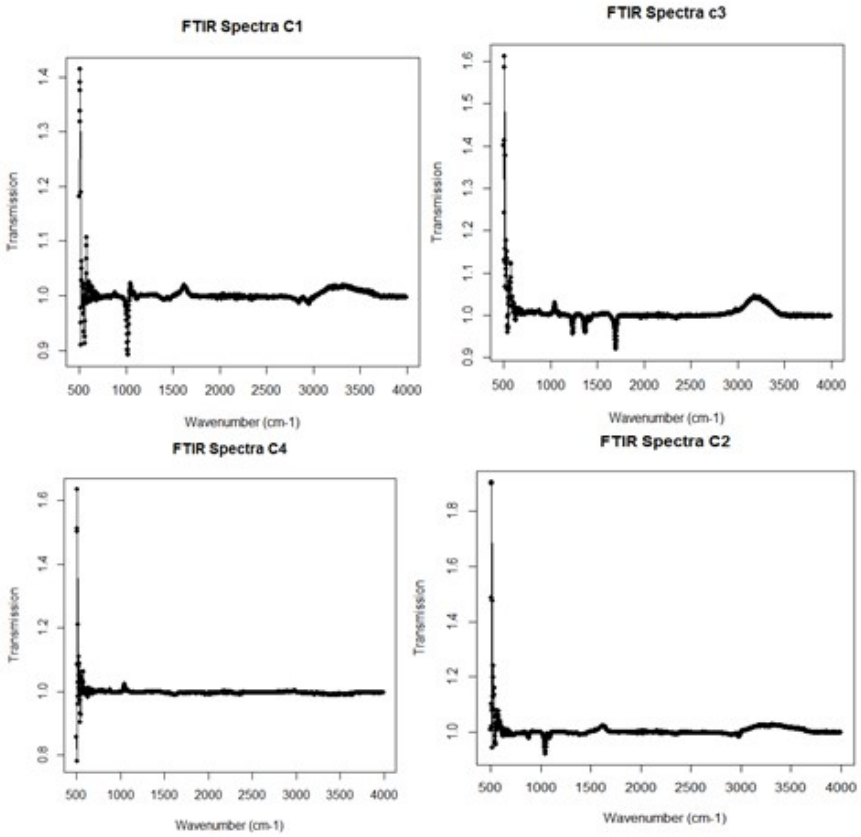

Fig. 3: Showed FTIR Spectra

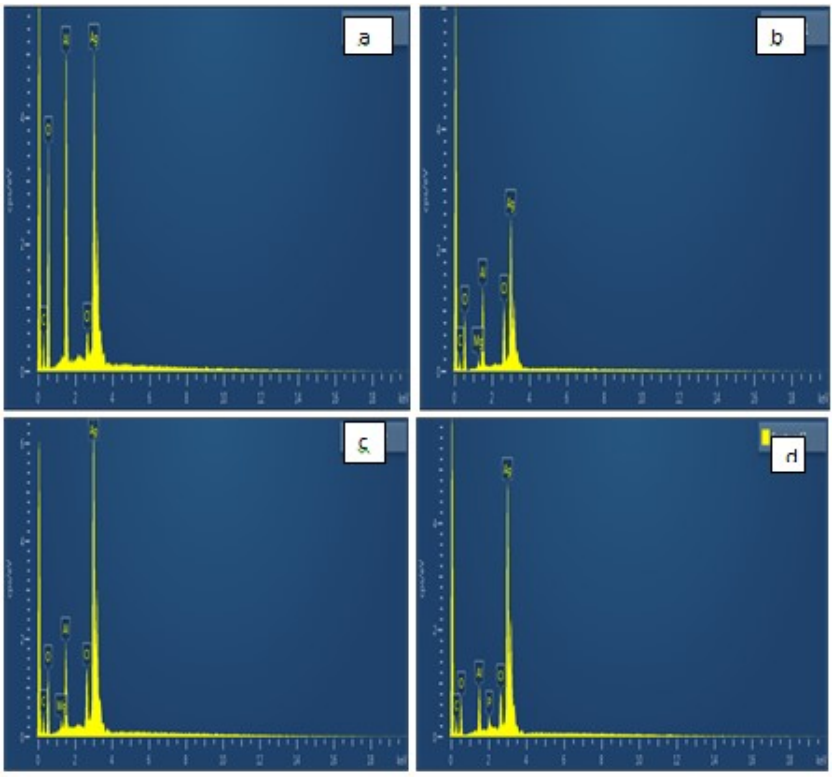

Fig. 4: Showed EDX analysis of biosynthesized SNPs (a) ethanol extract, (b) water extract,(c) methanol extract (d) acetone extract

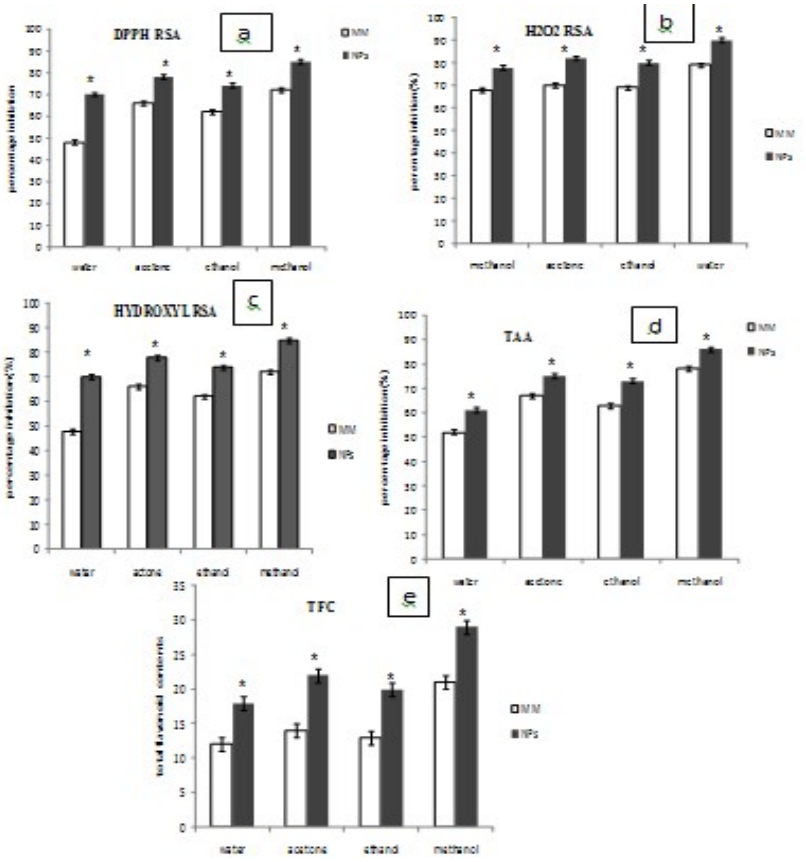

Fig. 5: Showed (a) prominent scavenging percentage of DPPH free radicals, (b) hydrogen peroxide free radicals, (c) hydroxyl radical, (d) phosphomolybdate free radical, (e) total flavonoids content

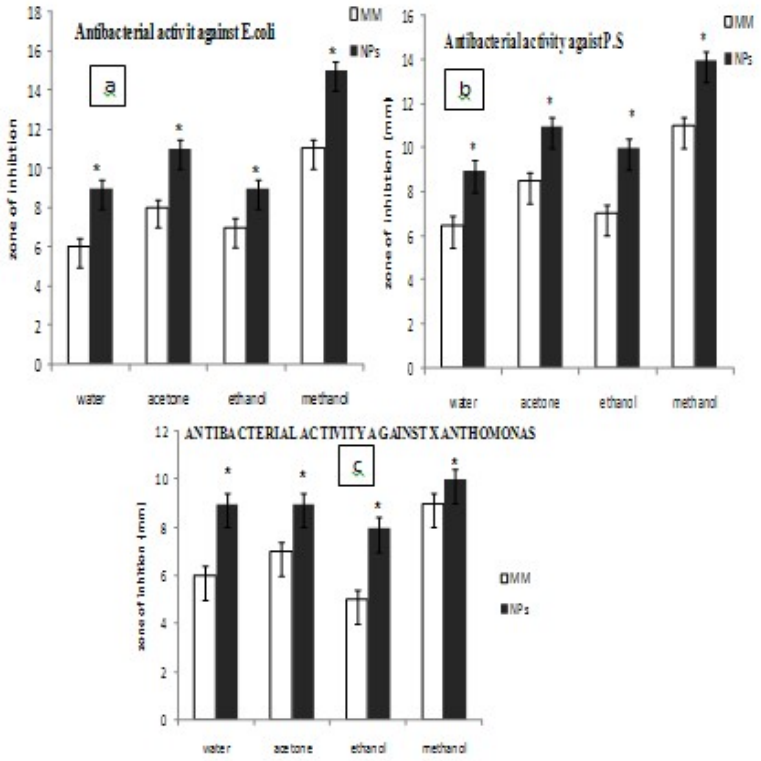

Fig. 6: Showed zone of inhibition against (a) E.coli, (b) pseudomonas syringae (c) Xanthomonas

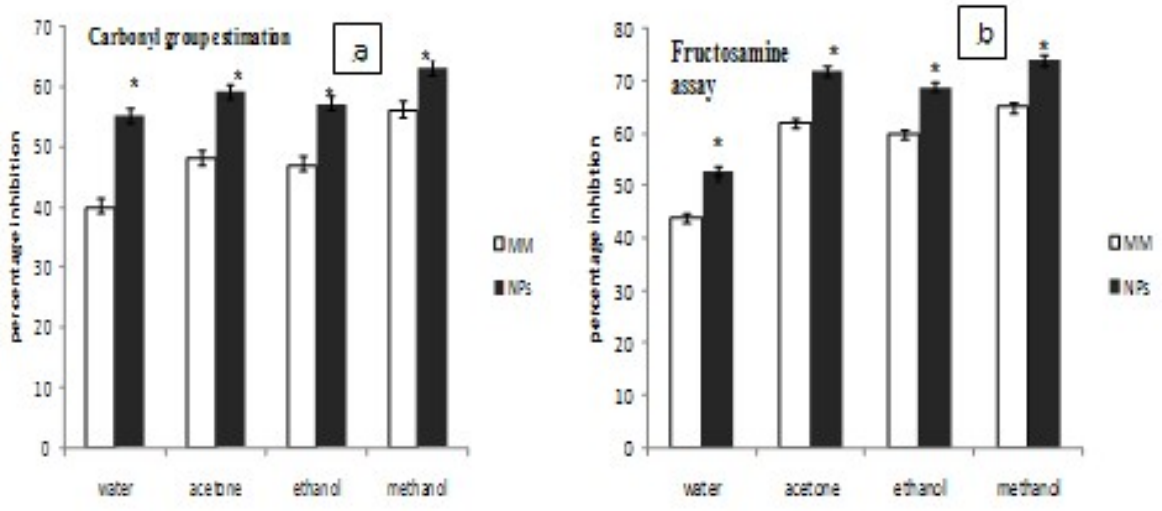

Fig. 7: showed Percentage inhibition of glycated material

Acetone and its respective nanoparticle (t=-7.730, P<0.05), ethanol and its respective nanoparticle (t=-5.016, P<0.05) and water and its respective nanoparticle (t=-7.626, P<0.05). Of the samples, nanoparticles of M.M. methanol extract exhibited substantially greater potential for scavenging than other specimens. There was a higher activity in the nanoparticles of all extracts than in crude.

Fig. 5e total flavonoid contents of (crude extracts and their respective NPs were evaluated by paired T test (df=1,4). The data showed the significant difference of methanol and its respective nanoparticle (t =-16.01, P<0.05), acetone and its respective NPs (t=-29.287, P<0.05), ethanol and its respective nanoparticle (t=-5.332, P<0.05) and water and its respective nanoparticle (t=-24.447, P<0.05). NPs of M.M. extract methanol have been shown to be of substantially higher content of flavonoids than those in all the samples. Percentage Inhibitions Nanoparticles ANOVA are tested two way: the approximate fructosamine test for crude extracts with their respective nanoparticles (df 1,4). The data showed the significant difference of methanol and its respective nanoparticles (t=-8.81, P<0.05), acetone and its respective nanoparticles (t=-7.426, P<0.05), ethanol and its respective nanoparticles (t=-9.501, P<0.05) and water and its respective nanoparticles (t=-13.079, P<0.05). Of all the samples, methanol extract nanoparticles were significantly more active than others. All extract nanoparticles have been more active than crude extracts.

Antimicrobial activity

Fig. 6a evaluates anova in two ways in the inhibitory zone for crude extracts and their respective nanoparticles. Extracts revealed a significant inhibitory zone. The findings indicated that M.M. ($F_{1,24}$ =61.272 p<0.05), NPs ($F_{1,24}$=88,926 p<0.05) and interaction between NPs and M.M. ($F_{1,24}$=14,765 p<0.05) had a substantial impact on each of these. The bigger zone among all the samples was shown by methanol extract nanoparticles. All extract nanoparticles exhibited greater areas than the raw extracts.

In Fig. 6b, anova was assessed by two means: the zone of inhibition and their nanoparticles of crude extracts. Extracts revealed a significant inhibitory zone. The findings indicated the important influence of crude extract M.M. ($F_{1,24}$=137.448 p<0.05), NP ($F_{1,24}$=45.656 p<0.05) and the interactions between MM and NP ($F_{1,24}$=18.978 p<0.05). The methanol extract nanoparticles exhibited the greater area than others in all the samples. There were larger zones of nanoparticles of all extracts than the crude extracts.

Fig. 6c evaluates the area of inhibition of raw extracts and their nanoparticles in two ways. Extracts revealed a significant inhibitory area. The findings revealed that the M.M. ($F_{1,24}$=57.176 p<0.05), NP ($F_{1,24}$=108.882 p<0.05) and MM/NP interaction ($F_{1,24}$=23.045 p<0.05) were significantly influenced. Among all samples, methanol extract NPs were found to be bigger than other samples. All extract's NPs exhibited larger areas than crude extracts.

Analysis of carbonyl group

Carbonyl group estimates for percentage inhibitions for crude extracts and their corresponding nanoparticles were assessed in two ways by anova. Extracts of fig. 7a demonstrated significant temporal inhibition. The findings indicated the substantial effects of MM ($F_{1,24}$= 114.03 p<0.05), NP ($F_{1,24}$= 88.07 p<0.05) and the interplay between MM and NP ($F_{1,24}$=18.307 p<0.05). Of all the samples, methanol extract nanoparticles have been much more active. All extract nanoparticles were more active than rough extracts.

Analysis of fructosamine

Two way anova has showed the percentage inhibits of the crude fructosamine assay and its respective nanoparticles (df 1, 24). In fig. 7b, the inhibition of fructosamine was evident in a time-sensitive way. The results indicated that MM ($F_{1,24}$ = 164.654 $p<0.05$). NP ($F_{1,24}$=102.67 $p<0.05$) and interaction ($F_{1,24}$= 199.379 $p<0.05$) were significant. The data demonstrated the meaningful effects. Nanoparticles of methanol extract were significantly more active than others across all samples. All extract nanoparticles were more active in comparison to crude extracts.

DISCUSSION

In our current study, the graph between absorption and the wavelength is shown in our current analysis in figs. 1a-1d. The metal ions were reduced easily. More than 90 percent reduction in silver ions has occurred after the metal ions have been applied to the factory. Ginova *et al*. (2013) were approximately 24 hours of maximum reduction in silver ions). Previous studies have shown that the height of SNPs (Gkogkolou *et al*., 2012) was about 400-450 nm.

Analysis is used for the identifying of functional groups by Fourier Transform Infrared Spectroscopy (FTIR). The stability of nanoparticles has also been established. Fig. 3a-3b displays the SNP biosynthesized FTIR spectrum. The FTIR set of SNPs showed the various bands. These groups demonstrate the various groups of functions. The band between the 3490-3500 cm-1 wave number shows the OH stretch. The OH bond is an alcoholic and phenolic complex. The peak of approximately 1,500-1,550 cm-1 showed (the spreading from C-H. (The maxim of approximately, 1450-1,500 cm-1 indicated the bond N-H. (The peak found approximately 500-550 cm-1 showed that the SNPs are extended (Halliwell. 1991). The vibration of the amino group was shown by the FTIR spectra. Therefore OH detention occurred on the surface of the NPs which contributed to the bactericidal effect of SNPs. Bacterial cell proteins bind to the SNPs. FTIR spectrum has been shown to be capped by proteins. The protein amino group helped to shape the SNPs. The amino group comprises a group of carbonyl. The carbonyl OH group caused silver ions to be reduced (Ho *et al*., 2010). The NPs were stabilized by the proteins. Therefore, in the biosynthesis of NPs the biomolecules did two functions. The silver ions were reduced. The NPs were stabilized. The flavonoids occur due to carbonyl group on the surface of the SNPs. In reducing silver ions, carbohydrate plays an important role. Reduction of sugars in the OH group caused silver metals to be reduced (Huh *et al*., 2011). Previous studies have shown that proteins are a reduction agent. The silver ions were reduced to SNPs (Javadi *et al*., 2017).

For qualitative and quantitative evaluation of different components, Electron diffraction X-Ray (EDX) is applied. The quantity of silver in the SNPs is calculated using the EDX. The different constituents of the plant with their respective nanoparticles against different bacteria used in our study Pseudomonas, *E. coli* and Xanthomas showed the prominent zone of inhibition that showed their property as an antibacterial agent. This study is similar with the findings of Srilatha and Ananda (2014) as they determined that several plant based biosynthesized SNPs are reported early. But the M.M. plant based SNPs are also reported too as it has high contents of phenolic compounds that have medicinal properties i.e. antibacterial, analgesic, stimulant and anti-inflammatory.

CONCLUSION

This study concluded that biosynthesized nanoparticles of M.M. plant peels extracts have the great biological activities i.e. antiglycation, antioxidant and antibacterial against Xanthomas, Pseudomonas and E.coli. In future prospective, more research is needed to know the exact dose rate and to compare the different dose combination of the plant with the strong antibiotic agents against these bacteria.

REFERENCES

Alexander JW (2009). History of the medical use of silver. *Surg Infections.,* **10**(3): 289-292.

Arsenopoulou ZV, Taitzoglou IA, Molyvdas PA, Gourgoulianis KI, Hatzoglou C and Zarogiannis SG (2018). Silver nanoparticles alter cell adhesion and proliferation of sheep primary mesothelial cells. *In vivo.,* **32**(1):109-112.

Balouiri M, Sadiki M and Ibnsouda SK (2016). Methods for *in vitro* evaluating antimicrobial activity: A review. *J. Pharmaceutical. Analysis,* **6**(2): 71-79.

Bhatia S (2016). Nanoparticles types, classification, characterization, fabrication methods and drug delivery applications. *In*: Natural. Polymer. Drug Delivery Systems (Springer), pp. 33-93.

Bose A, Bose S, Maji S and Chakraborty P (2009). Free radical scavenging property of *Quisqualis indica*. *Int. J. Biomedical. Pharmaceutical. Sci.,* **3**(1): 1-4.

Chitra G, Balasubramani G, Ramkumar R, Sowmiya R and Perumal P (2015). *Mukia maderaspatana* (Cucurbitaceae) extract-mediated synthesis of silver nanoparticles to control *Culex quinquefasciatus* and *Aedes aegypti* (Diptera: Culicidae). *Parasitol Res.,* **114**(4): 1407-1415.

Chang ST, Wu JH, Wang SY, Kang PL, Yang NS and Shyur LF (2001). Antioxidant activity of extracts from *Acacia confusa* bark and heartwood. *J. Agricultural Food Chem.,* **49**(7): 3420-3424.

Dadfar SM, Roemhild K, Drude NI, von Stillfried S, Knüchel R, Kiessling F and Lammers T (2019). Iron

oxide nanoparticles: Diagnostic, therapeutic and theranostic applications. *Adv. Drug Deliv. Rev.,* **138**: 302-325.

Devi GK and Sathishkumar K (2016). Synthesis of gold and silver nanoparticles using *Mukia maderaspatna* plant extract and its anticancer activity. *IET Nanobiotechnol.,* **11**(2): 143-151.

De Filippo C, Cavalieri D, Di Paola M, Ramazzotti M, Poullet JB, Massart S and Lionetti P (2010). Impact of diet in shaping gut microbiota revealed by a comparative study in children from Europe and rural Africa. *Proceedings of the National Academy of Sciences,* **107**(33): 14691-14696.

Dipankar C and Murugan S (2012). The green synthesis, characterization and evaluation of the biological activities of silver nanoparticles synthesized from Iresine herbstii leaf aqueous extracts. *Colloids Surfaces B: Biointerfaces.,* **98**: 112-119.

Durán N, Marcato PD, Alves OL, De Souza GI and Esposito E (2005). Mechanistic aspects of biosynthesis of silver nanoparticles by several *Fusarium oxysporum* strains. *J. Nanobiotechnol.,* **3**(1): 8.

Firdhouse MJ and Lalitha P (2015). Biosynthesis of silver nanoparticles and its applications. *J. Nanotechnol.,* p.18.

Giacco F and Brownlee M (2010). Oxidative stress and diabetic complications. *Circulation Res.,* **107**(9): 1058-1070.

Ginova A, Mihalev K and Kondakova V (2013). Antioxidant capacity of petals and leaves from different rose. *Int. J. Pure. App. Biosci.,* **1**(2): 38-43.

Gurunathan S, Raman J, Malek SNA, John PA and Vikineswary S (2013). Green synthesis of silver nanoparticles using Ganoderma neo-japonicum Imazeki: A potential cytotoxic agent against breast cancer cells. *Int. J. Nanomedicine.,* **8**: 4399.

Gkogkolou P and Bohm M (2012). Advanced glycation end products: Key players in skin aging? *Dermato-endocrinology.,* **4**(3): 259-270.

Guzman M, Dille J and Godet S (2012). Synthesis and antibacterial activity of silver nanoparticles against gram-positive and gram-negative bacteria. *Nanomedicine: Nanotechnol, Biol Med.,* **8**(1): 37-45.

Halliwell B (1991). Reactive oxygen species in living systems: Source, biochemistry, and role in human disease. *The Am. J. Med.,* **91**(3): S14-S22.

Ho SC, Wu SP, Lin SM and Tang YL (2010). Comparison of anti-glycation capacities of several herbal infusions with that of green tea. *Food Chem.,* **122**(3): 768-774.

Huh AJ and Kwon YJ (2011). Nanoantibiotics: A new paradigm for treating infectious diseases using nanomaterials in the antibiotics resistant era. *J. Controlled Release.,* **156**(2): 128-145.

Javadi B, Sahebkar A and Emami SA (2017). Medicinal plants for the treatment of asthma: A traditional persian medicine perspective. *Curr. Pharm. Des.,* **23**(11): 1623-1632.

Kaewnarin K, Niamsup H, Shank L and Rakariyatham N (2014). Antioxidant and antiglycation activities of some edible and medicinal plants. *Chiang Mai J. Sci.,* **41**(1): 105-116.

Kasthuri J, Veerapandian S and Rajendiran N (2009). Biological synthesis of silver and gold nanoparticles using apiin as reducing agent. *Colloids and Surfaces B: Biointerfaces.,* **68**(1): 55-60.

Kumar A, Vemula PK, Ajayan PM and John G (2008). Silver-nanoparticle-embedded antimicrobial paints based on vegetable oil. *Nature materials.,* **7**(3): 236.

Kumar RS, Rajkapoor B and Perumal P (2012). Antioxidant activities of *Indigofera cassioides* Rottl. Ex. DC. using various *in vitro* assay models. *Asian Pacific J. Tropical Biomedicine.,* **2**(4): 256.

Khan M, Tareq F, Hossen M and Roki M (2018). Green synthesis and characterization of silver nanoparticles using *Coriandrum sativum* leaf extract. *J. Engg. Sci. Technol.,* **13**(1): 158-166.

Khatami M, Sharifi I, Nobre MA, Zafarnia N and Aflatoonian MR (2018). Waste-grass-mediated green synthesis of silver nanoparticles and evaluation of their anticancer, antifungal and antibacterial activity. *Green Chem. Letter Reviews.,* **11**(2): 125-134.

Kuppusamy P, Yusoff MM, Maniam GP and Govindan N (2016). Biosynthesis of metallic nanoparticles using plant derivatives and their new avenues in pharmacological applications–An updated report. *Saudi Pharm J.,* **24**(4): 473-484.

Lin Z, Monteiro Riviere NA and Riviere JE (2015). Pharmacokinetics of metallic nanoparticles. Wiley Interdisciplinary Reviews: *Nanomedicine Nano-biotechnol.,* **7**(2): 189-217.

Liu WT (2006). Nanoparticles and their biological and environmental applications. *J. Biosci. Bioengineering.,* **102**(1): 1-7.

Lalitha P, Sripathi SK and Jayanthi P (2012). Secondary metabolites of *Eichhornia crassipes* (Waterhyacinth): A review (1949 to 2011). *Nat. Prod. Commun.,* **7**(9): 1249-1256.

Logeswari P, Silambarasan S and Abraham J (2015). Synthesis of silver nanoparticles using plants extract and analysis of their antimicrobial property. *J. Saudi Chem. Society.,* **19**(3): 311-317.

McPherson JD, Shilton BH and Walton DJ (1988). Role of fructose in glycation and cross-linking of proteins. *Biochemistry,* **27**(6): 1901-1907.

Mehta B, Chhajlani M and Shrivastava B (2017). Green synthesis of silver nanoparticles and their characterization by XRD. *J. Phys. Conf. Ser.,* **836**(1): 012050.

Moodley JS, Krishna SBN, Pillay K and Govender P (2018). Green synthesis of silver nanoparticles from *Moringa oleifera* leaf extracts and its antimicrobial potential. *Advances Natural Sci*. *Nanosci Nanotechnol*., **9**(1): 015011.

Perugu S, Nagati V and Bhanoori M (2016). Green synthesis of silver nanoparticles using leaf extract of medicinally potent plant *Saraca indica:* A novel study. *App Nanosci.,* **6**(5): 747-753.

Petrus A (2013). Ethnobotanical and pharmacological profile with propagation strategies of *Mukia maderaspatana* (L.) M. Roem. A concise overview. *Ind. J. Natural Products Resources,* **4**(1):9-26

Prieto P, Pineda M and Aguilar M (1999). Spectro-photometric quantitation of antioxidant capacity through the formation of a phosphomolybdenum complex: Specific application to the determination of vitamin E. *Anal Biochem.,* **269**(2): 337-341.

Qidwai A, Kumar R and Dikshit A (2018). Green synthesis of silver nanoparticles by seed of *Phoenix sylvestris* L. and their role in the management of cosmetics embarrassment. *Green Chem Letters Rev.,***11**(2): 176-188.

Rao NH, Lakshmidevi N, Pammi S, Kollu P, Ganapaty S and Lakshmi P (2016). Green synthesis of silver nanoparticles using methanolic root extracts of *Diospyros paniculata* and their antimicrobial activities. *Mat. Sci. Engineering. C,* **62**: 553-557.

Ruch RJ, Cheng SJ and Klaunig JE (1989). Prevention of cytotoxicity and inhibition of intercellular communication by antioxidant catechins isolated from Chinese green tea. *Carcinogenesis,* **10**(6): 1003-1008.

Sabourian P, Yazdani G, Ashraf SS, Frounchi M, Mashayekhan S, Kiani S and Kakkar A (2020). Effect of physico-chemical properties of nanoparticles on their intracellular uptake. *Int. J. Mol. Sci.,* **21**(21): 8019.

Sarkar S and Kotteeswaran V (2018). Green synthesis of silver nanoparticles from aqueous leaf extract of pomegranate (*Punica granatum*) and their anticancer activity on human cervical cancer cells. *Adv. Nat. Sci.: Nanosci. Nanotechnol.,* **9**(2): 025014.

Shah M, Fawcett D, Sharma S, Tripathy S and Poinern G (2015). Green synthesis of metallic nanoparticles via biological entities. *Materials.,* **8**(11): 7278-7308.

Shaik M, Khan M, Kuniyil M, Al-Warthan A, Alkhathlan H, Siddiqui M and Khan M (2018). Plant-extract-assisted green synthesis of silver nanoparticles using *Origanum vulgare* L. extract and their microbicidal activities. *Sustainability,* **10**(4): 913.

Soares MR, Corrêa RO, Stroppa PHF, Marques FC, Andrade GF, Correa CC and Raposo NR (2018). Biosynthesis of silver nanoparticles using *Caesalpinia ferrea* (Tul.) Martius extract: Physicochemical characterization, antifungal activity and cytotoxicity. *Peer. J.,* **6**: e4361.

Srilatha B and Ananda S (2014). Antidiabetic effects of Mukia maderaspatana and its phenolics: An *in vitro* study on gluconeogenesis and glucose uptake in rat tissues. *Pharmaceutical. Biol*., **52**(5): 597-602.

Zargar M, Hamid AA, Bakar FA, Shamsudin MN, Shameli K, Jahanshiri F and Farahani F (2011). Green synthesis and antibacterial effect of silver nanoparticles using *Vitex negundo* L. *Molecules.,* **16**(8): 6667-6676.

Zhang H (2020). Molecularly imprinted nanoparticles for biomedical applications. *Adv. Mater.,* **32**(3): e1806328.